

Hirshfeld Surface and Natural Bond Orbital Analysis of 2-Amino-6-Methylpyridinium Hydrogen Glutarate

S. Nithya*, Assistant Professor, Department of Physics, Kumaraguru College of Technology, Coimbatore, India, nithyvj@gmail.com

B. Chandar Shekar, Assistant Professor, Department of Physics, Kongunadu Arts and Science College, Coimbatore, India, Chandar.bellan@gmail.com

K.R. Aranganayagam, Assistant Professor, Department of Chemistry, Kumaraguru College of Technology, Coimbatore, India, aranganayagam@gmail.com

K. Boopathi, DST Inspire faculty, School of Chemical Science, Department of Inorganic Chemistry, University of Madras (Guindy Campus), India, boopathibp@gmail.com

Abstract: Single crystals of 2- Amino-6-methylpyridinium hydrogen glutarate (2A6MPHG) have been grown by slow evaporation technique. From the single crystal X-ray diffraction studies, it was found that the crystal belongs to orthorhombic crystal system with the non-centrosymmetric space group $P2_12_12_1$. The presence of various proton and carbon positions in the crystal was confirmed using ^1H NMR and ^{13}C NMR spectral studies. The thermal stability of the crystal was determined by TG/DTA analysis. The optical behavior of the crystal was examined by photoluminescence studies. The quantum chemical calculations on 2A6MPHG have been performed by density functional theory (DFT) calculations using the B3LYP method with 6-31 G (d,p) basis set. The Hirshfeld surface analysis, Mulliken charge, Molecular electrostatic potential and Natural bond orbital analysis (NBO) for 2A6MPHG has been studied.

Keywords: *Slow evaporation, non-centrosymmetric, NMR, DFT, Hirshfeld, NBO*

I. INTRODUCTION

Nonlinear optical (NLO) materials have fascinating properties which makes it suitable in different applications like laser technology, photonics and terahertz generation [1]-[4]. Inorganic crystals in spite of having high mechanical strength are poor in optical nonlinearity. In order to improve the nonlinearity of the material, organic crystals having wide transparency and high resistance to optical damage were employed. Optical nonlinearity is more in organic crystals than the inorganic counterpart owing to the presence of weak Vander Waals and hydrogen bonds. In connection to this semiorganic materials are of great interest in molecular engineering as they provide many interesting structure and bonding schemes. The optical nonlinearity arises from the π -electron behaviour due to the insertion of an inorganic unit in a conjugated structure [5]. Larger value of hyperpolarizability which is an effective tool for nonlinear response ascends due to the ability of the molecule to form inter- and intramolecular interactions. The close packing of molecules by hydrogen bonding contributes to the efficient nonlinear optical crystals. Such crystals have high optical data storage, optical memory, frequency shifting which finds applications in signal

processing and optical communications [6]-[8]. Pyridine, one of the simplest heteroaromatic compounds, has four independent molecules in the asymmetric unit. Pyridine based derivatives exhibit effective nonlinear response. Previously, Sergiu Draguta et al reported the crystal structure of 2-amino-6-methylpyridinium hydrogen glutarate (2A6MPHG) [9]. A thorough review postulates that there is no further characterization results were carried out for this material. In this context 2-amino-6-methylpyridinium hydrogen glutarate (2A6MPHG) a semiorganic crystal has been grown and characterized by single crystal XRD, NMR, TG/DTA and photoluminescence study. Theoretical investigations such as, Hirshfeld analysis, Mulliken charge studies, molecular electrostatic potential and natural bond orbital analysis were also carried out by density functional calculations based on Becke-3-Lee-Yang-Parr (B3LYP) with the B3LYP/6-31G level employed in the GAUSSIAN 09 program suite.

II. EXPERIMENTAL

Stoichiometric (1:1) ratio of the reactants 2-amino-6-methylpyridine and glutaric acid were dissolved in methanol. To obtain a homogeneous mixture the prepared

solution was stirred well for about 5 hours using a magnetic stirrer. During the reaction, a proton is transferred from the electron donor group of glutaric acid to the electron acceptor group of 2-amino 6-methylpyridine resulting 2-amino-6- methylpyridinium hydrogen glutarate compound. Then the solution was filtered by whatmann filter paper to a beaker and allowed to evaporate slowly. 2-amino-6-methylpyridinium hydrogen glutarate crystals (Figure 1) were obtained after a period of 30 days.

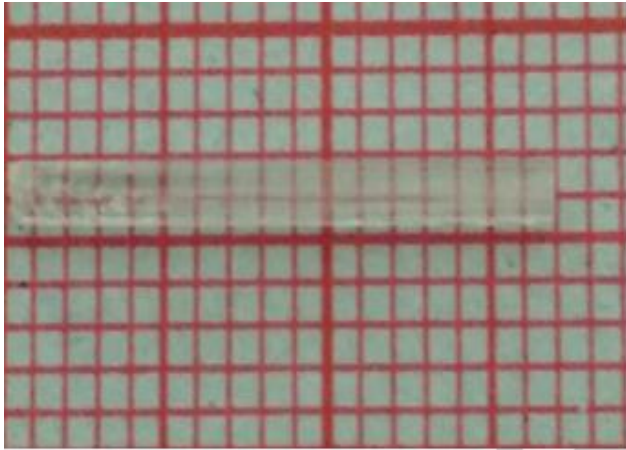


Fig. 1. Crystal Photograph of 2A6MPHG

III. CHARACTERIZATION

The single crystal of 2A6MPHG obtained was subjected to single crystal X-ray Diffraction studies using a Bruker AX diffractometer with $\text{MoK}\alpha$ ($\lambda = 0.71073 \text{ \AA}$) radiation. ^1H NMR and ^{13}C NMR spectra were recorded employing a Bruker 500 MHz spectrometer in deuterated solvent, using DMSO in order to confirm the title compound. Thermogravimetric analysis (TGA) and differential thermal analysis (DTA) experiments were carried out by Elmer simultaneous thermogravimetric and differential thermal (TGA & DTA) analyzers with a heating rate of $10 \text{ }^\circ\text{C}/\text{min}$ from 20 to $400 \text{ }^\circ\text{C}$ in an inert nitrogen atmosphere. Photoluminescence study for 2A6MPHG was analysed using JASCO spectrofluorophotometer. Theoretical investigations such as Hirshfeld analysis, molecular electrostatic potential, Mulliken charge studies, and natural bond analysis were also carried out by density functional calculations based on Becke-3-Lee-Yang-Parr (B3LYP) with the B3LYP/6-31 G level employed in the GAUSSIAN 09 program suite.

IV. RESULTS AND DISCUSSION

Single crystal X-ray diffraction studies

X-ray powder diffraction was used to identify the lattice parameters of 2A6MPHG crystal which is subjected to Bruker AX diffractometer with $\text{MoK}\alpha$ ($\lambda = 0.71073 \text{ \AA}$) radiation. The 2A6MPHG crystal belongs to the orthorhombic crystal system with the non-centrosymmetric space group $\text{P}2_12_12_1$. The lattice parameters obtained in the

present study are found to be $a = 5.2263 \text{ \AA}$, $b = 11.07 \text{ \AA}$, $c = 23.53 \text{ \AA}$, $\alpha = \beta = \gamma = 90^\circ$ and the unit cell volume is 1165 \AA^3 which agrees with the previous work [9].

NMR Spectral analysis

Nuclear magnetic resonance (NMR) is a potential technique used for the identification of organic compounds. The recorded ^1H and ^{13}C NMR spectra (δ in ppm) are shown in figures 2a and 2b, respectively. In ^1H NMR, the peak appearing at 2.51 ppm is attributed to methyl proton in the 2-amino-6-methylpyridinium moiety. The peak at 6.33 ppm is due to the proton of NH_2 in the 2-amino-

6-methylpyridinium moiety. In ^{13}C spectrum, the carbon attached to nitrogen atom could be observed at the signals $\delta = 137.96$ and 156 ppm respectively. The peak at 174.67 ppm could be attributed to the carbon atom in carboxylate group. This confirms the compound formation of 2A6MPHG.

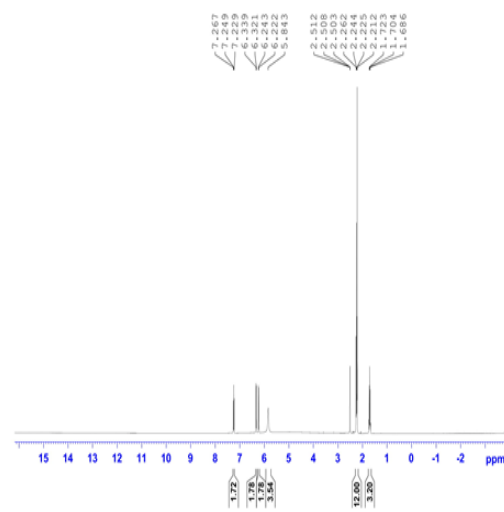


Fig.2a. ^1H NMR spectrum of 2A6MPHG

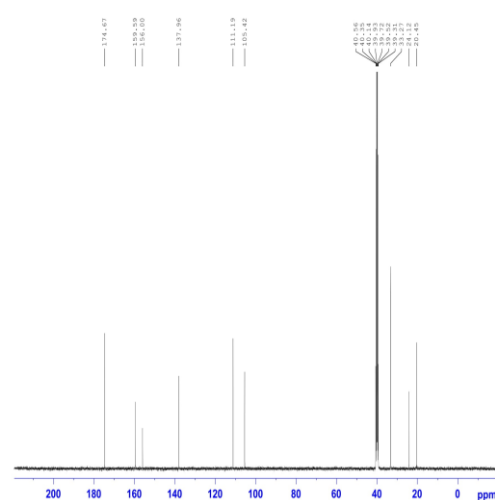


Fig.2b. ^{13}C NMR spectrum of 2A6MPHG

TG/DTA analysis

The TG/DTA curve for 2A6MPHG is shown in figure 3. From the TG curve, single stage decomposition is observed and major weight loss occurs from 128°C to 246°C. It shows that the compound is stable up to 128°C and the decomposition continues up to 700°C. From DTA curve, two endothermic peaks were observed. The

peak at 143°C is assigned to the absorption of energy for the breaking of bonds at the initial stage of decomposition and the second peak at 223 °C is assigned to the melting of the compound. From the TG/DTA results, it is concluded that 2A6MPHG crystals can be used for NLO and laser applications.

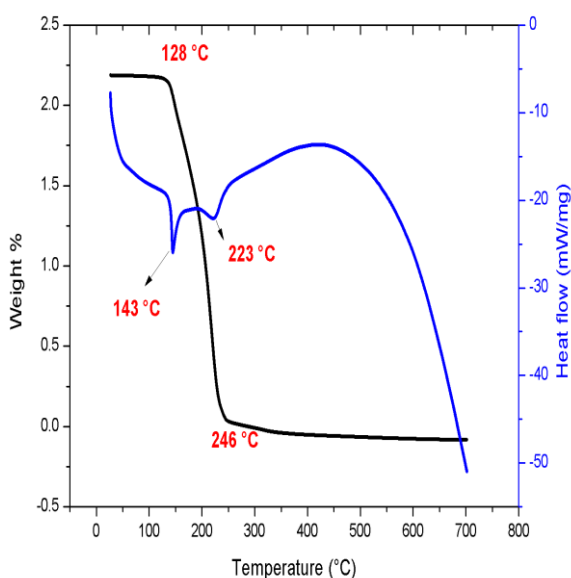


Fig.3. TGA and DTA curve of 2A6MPHG

Photoluminescence studies

Photoluminescence spectroscopy which is a non-destructive technique provides information regarding material characterization for semiconductor device fabrication [10]. The photoluminescence emission spectrum is shown in figure 4. The intensity peak at 379.6 nm could be due to the $n \rightarrow \pi^*$ transitions present in the 2A6MPHG crystal. These transitions may be attributed to the intermolecular interaction due to the protonation of nitrogen.

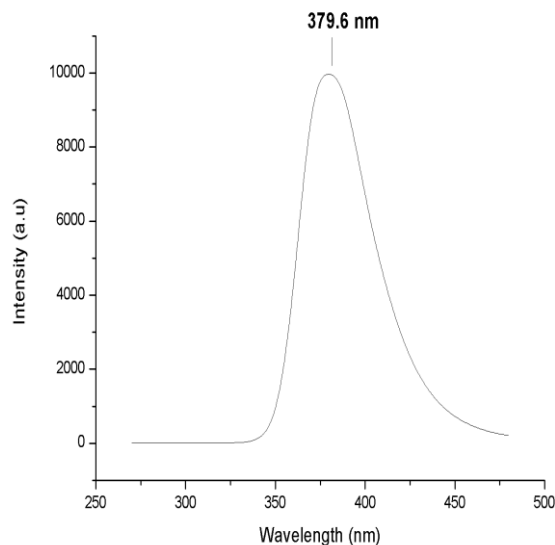


Fig. 4. Photoluminescence spectrum

Hirshfeld Surface Analysis

Hirshfeld surface analysis is a useful tool for the investigation of intermolecular interactions. From the three-dimensional contour plots and two-dimensional fingerprint plots in Hirshfeld analysis, the intermolecular interactions are visualized. The hydrogen bonding interactions as well as π - π interactions are evident from 2D fingerprint plots. The Hirshfeld surfaces of 2A6MPHG are given in the figure 5b showing the surfaces that have been mapped over d_i (0.645 to 2.376 Å), d_e (0.645 to 2.331 Å), d_{norm} (-0.745 to 1.186 Å), shape index (-1.0 to 1.0 Å) and curvedness (-4.0 to +4.0 Å). The color coding in the crystal represents the intermolecular interactions [11]. The d_{norm} surface is displayed using red-white-blue colour scheme in which red colour highlights the short contact, while white colour indicates van der Waals separation and blue for longer contacts [12]. The bright red spots represented by circular depressions in d_{norm} surface correspond to N-H...O interactions between amino group and oxygen atom of hydrogen glutarate whereas the light red areas are due to C-H...O interactions. The shape index surface indicates the presence of π - π stacking interactions present in the crystal from adjacent red and blue triangles. The π - π stacking interactions are also evident from the flat region in curvedness. In 2D plot, the H...H contacts which appear as distinct spikes, shown in figure 5a, have a most significant contribution to the total Hirshfeld surfaces (42.3%). The relative contributions for other interactions are H...O, C...H, N...H, C...N and C...C contacts are 41.5 %, 12.5 %, 2.7 %, 0.8 % and 0.2 %.

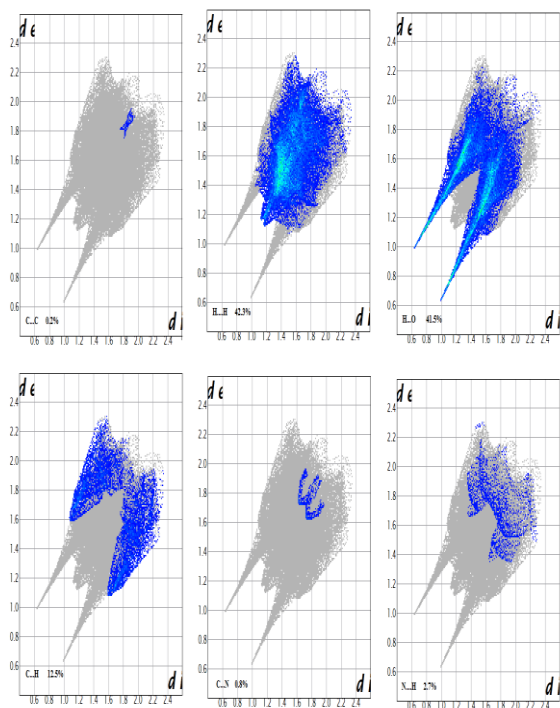


Fig. 5(a) Fingerprint plots of 2A6MPHG

highest value of positive charge of 0.4549e. Among oxygen atoms O1 shows highest value of electronegativity of -0.52672e. The highest value of hydrogen and oxygen atoms could be attributed to N-H...O interactions.

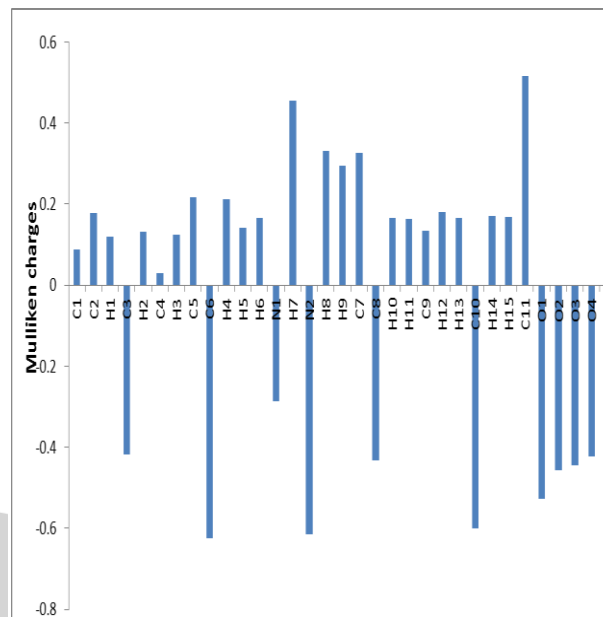


Fig. 6. Mulliken atomic charges plot of 2A6MPHG

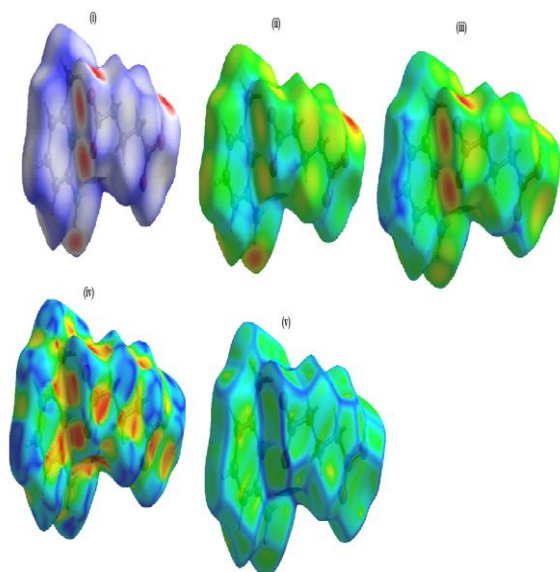


Fig. 5(b) Hirshfeld surfaces mapped on i) dnorm ii) di iii) de iv) shape index and v) curvedness

Mulliken charge analysis

Mulliken population method could be useful in the calculation of the reactive behavior of chemical systems in both electrophilic and nucleophilic reactions [13]. The charge distribution on various atoms of 2A6MPHG is plotted and shown in figure 6. It is evident from mulliken charge distribution that the carbon atoms C1, C2, C4 and C5 in pyridine ring are positively charged and the carbon atoms C3 and C6 are negatively charged. The hydrogen atom H7 involved in intermolecular interactions shows the

Molecular electrostatic potential

The molecular electrostatic potential (MEP) is used to explore the interactions present in the molecule. The electrostatic potential contour map of 2A6MPHG molecule is shown in figure 7. The negative potential regions are related to electrophilic reactivity, while the positive potential regions are related to nucleophilic reactivity. To label the different electron density sites in the molecule, different colour codes are used in electrostatic maps.

The maximum negative region, which is the electrophilic site, is depicted as red, while the maximum positive region, which is the nucleophilic site, is depicted as blue. For the investigation of the physiochemical property relationships of molecular structures, electrostatic potential contour maps are used [14], [15]. The regions of red in 2A6MPHG molecule which are characterized as negative electrostatic potential were localized on the oxygen atoms of hydrogen glutarate and this region acts as electrophilic centres. The positive regions are related to nucleophilic centers and are mainly localized over the pyridinium molecule.

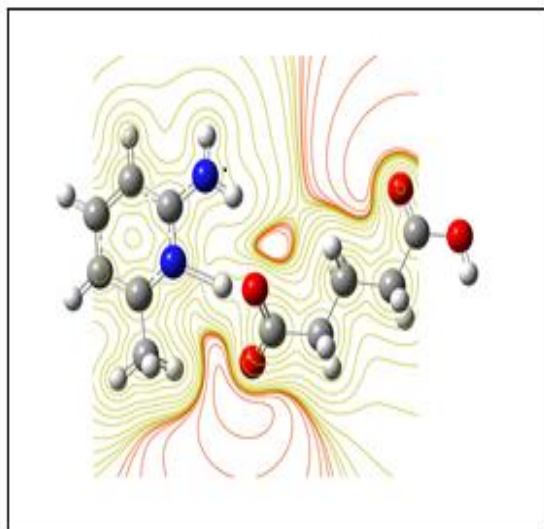


Fig. 7. Electrostatic potential contour map

NBO Analysis

NBO analysis is a suitable method for studying intra and intermolecular bonding and also provides a convenient basis for investigation of charge transfer or conjugative interactions in molecular system [16]. The larger the $E(2)$ value, the more intensive is the interaction between electron donors and the greater the extent of conjugation of the whole system. The NBO analysis results are listed in Table 1.

Table 1: Second order perturbation theory analysis of Fock matrix in NBO using DFT at B3LYP/6-31 G (d,p) level for 2A6MPHG

Donor	Acceptor	$E(2)$ Kcal/mol	$E(j)-E(i)$ a.u	$F(i,j)$ a.u
σ C1 - C2	σ^* C1 - N13	1.72	1.23	0.041
σ C1 - N13	σ^* C1 - C2	1.93	1.36	0.046
π C1 - N13	π^* C6 - C8	27.99	0.34	0.089
σ C1 - N15	σ^* C1 - C2	1.15	1.35	0.035
σ C2 - H3	σ^* C1 - N13	5.29	1.05	0.067
σ C2 - H3	σ^* C4 - C6	3.49	1.1	0.055
σ C2 - C4	σ^* C1 - C2	2.24	1.24	0.047
σ C2 - C4	σ^* C1 - N15	4.15	1.17	0.062
σ C2 - C4	σ^* C2 - H3	1.46	1.17	0.037
π C2 - C4	π^* C1 - N13	29.78	0.25	0.082
π C2 - C4	π^* C6 - C8	12.78	0.29	0.055
σ C4 - H5	σ^* C1 - C2	3.43	1.06	0.054
σ C4 - C6	σ^* C6 - C8	2.37	1.27	0.049
σ C6 - H7	σ^* C2 - C4	3.32	1.1	0.054
σ C6 - C8	σ^* C4 - H5	2.39	1.17	0.047
π C6 - C8	π^* C1 - N13	12.13	0.24	0.05
π C6 - C8	π^* C2 - C4	26.46	0.28	0.077
σ C8 - N13	σ^* C1 - N13	1.51	1.35	0.04

σ C9 - H11	σ^* C8 - N13	4.89	1.02	0.063
σ C9 - H12	σ^* C6 - C8	1.59	1.06	0.037
σ C9 - H12	π^* C6 - C8	4.37	0.52	0.046
σ N15 - H16	σ^* C1 - C2	4.35	1.19	0.064
σ N15 - H17	σ^* C1 - N13	4.83	1.18	0.068
LP (1) N13	σ^* C1 - C2	9.09	0.88	0.083
LP (1) N13	σ^* C1 - N15	3.81	0.81	0.051
LP (1) N15	π^* C1 - N13	43.93	0.27	0.105
π^* C1 - N13	π^* C2 - C4	107.2	0.03	0.083
π^* C1 - N13	π^* C6 - C8	67.18	0.04	0.074
π^* C6 - C8	σ^* C9 - H10	0.65	0.45	0.038
π^* C6 - C8	σ^* C9 - H12	1.09	0.41	0.047
σ C1 - C2	LP*(1) H14	0.24	0.85	0.014
σ C1 - N13	LP*(1) H14	1.23	0.98	0.035
π C1 - N13	LP*(1) H14	0.4	0.45	0.013
σ C6 - C8	LP*(1) H14	0.28	0.85	0.016
σ C8 - N13	LP*(1) H14	1.08	0.97	0.033
σ C9 - H10	LP*(1) H14	0.12	0.63	0.009
σ N15 - H16	LP*(1) H14	0.29	0.8	0.016
LP (1) N13	LP*(1) H14	61.55	0.49	0.169
π^* C1 - N13	LP*(1) H14	0.43	0.15	0.01
LP*(1) H14	σ^* C1 - C2	0.07	0.39	0.009
π C18 - O30	σ^* C9 - H10	0.08	0.85	0.007
LP (1) O29	σ^* N15 - H16	0.91	1.03	0.028
σ C18 - O29	LP*(1) H14	12.98	1.06	0.12
σ C18 - O30	LP*(1) H14	0.31	1.21	0.02
LP (1) O29	LP*(1) H14	13.05	0.69	0.096
LP (3) O29	LP*(1) H14	374.52	0.66	0.455

The results indicates that the hydrogen bonding interactions are formed between lone pairs (LP) of oxygen and antibonding σ^* orbitals of (N-H) which is evident from the interactions LP1 (O29) \rightarrow σ^* (N15-H16) associated with stabilization energy of 0.91 kcal/mol respectively. The most dominant charge transfer interactions in 2A6MPHG is LP3 (O29) \rightarrow LP*(1)(H14) with the highest delocalization energy of 374.52 kcal/mol. Further the interactions π (C2-C4) \rightarrow π^* (C1-N13), π (C1-N13) \rightarrow π^* (C6-C8), π (C6-C8) \rightarrow π^* (C1-N13), and π (C6-C8) \rightarrow π^* (C2-C4) with stabilization energy 29.78 kcal/mol, 27.99 kcal/mol, 12.13 kcal/mol and 26.46 kcal/mol respectively contributes stronger stabilization to the structure.

V. CONCLUSION

Nonlinear optical single crystals 2A6MPHG are grown by slow solvent evaporation method. Single crystal X-ray diffraction studies revealed that the grown crystal belongs to orthorhombic crystal system with space group $P2_12_12_1$. The identification of various protons and carbons in the

compound were assigned by ^1H and ^{13}C NMR spectral technique. From the thermal studies, it is evident that the crystal was stable up to 128°C . Photoluminescence study was carried out for the crystal. The quantum chemical calculations such as Hirshfeld analysis, Mulliken charge distribution, Electrostatic potential contour map and NBO analysis were carried out for the title compound. In 2A6MPHG, Hirshfeld surface analysis was used to study the interactions present in the compound and the charge distribution among the atoms is analysed by the electrostatic potential contour map. NBO analysis revealed intermolecular interactions in the molecular system of 2A6MPHG. Hence, it is concluded that that the 2A6MPHG crystal is suitable for NLO applications.

REFERENCES

- [1] Ma, X. F., and X-C. Zhang. "Determination of ratios between nonlinear-optical coefficients by using subpicosecond optical rectification." *JOSA B* Vol. 10, no. 7 pp.1175-1179, 1993, doi.org/10.1364/JOSAB.10.001175
- [2] Periyasamy, Bhuvana K., Robinson S. Jebas, and Balasubramanian Thailampillai. "Synthesis and spectral studies of 2-aminopyridinium para-nitrobenzoate: A novel optoelectronic crystal." *Materials Letters* Vol. 61, no. 7 pp.1489-1491, 2007.doi.org /10.1016/j.matlet.2006.07.069
- [3] Prasad, Paras N., and David J. Williams. *Introduction to nonlinear optical effects in molecules and polymers*. Vol. 1. New York etc.: Wiley, 1991.
- [4] Caroline, M. Lydia, and S. Vasudevan. "Growth and characterization of an organic nonlinear optical material: L-alanine alaninium nitrate." *Materials Letters*, Vol. 62, no. 15,pp.2245-2248, 2008.
- [5] Jiang, Min-hua, and Qi Fang. "Organic and semiorganic nonlinear optical materials." *Advanced Materials*, Vol. 11, no. 13, pp.1147-1151, 1999.
- [6] Dmitriev, Valentin G., Gagik G. Gurzadyan, and David N. Nikogosyan. *Handbook of nonlinear optical crystals*. Vol. 64. Springer, 2013.
- [7] Razzetti, C., M. Ardoino, L. Zanotti, M. Zha, and C. Paorici. "Solution growth and characterisation of L-alanine single crystals." *Crystal Research and Technology: Journal of Experimental and Industrial Crystallography*, Vol. 37, no. 5, pp.456-465, 2002.
- [8] Wong, Man Shing, Christian Bosshard, Feng Pan, and Peter Günter. "Non-classical donor-acceptor chromophores for second order nonlinear optics." *Advanced Materials*, Vol.8, no. 8, pp. 677-680, 1996.
- [9] Draguta, Sergiu, Marina S. Fonari, Shabari Nath Bejagam, Kathryn Storms, Jennifer Lindline, and Tatiana V. Timofeeva. "Structural similarities and diversity in a series of crystalline solids composed of 2-aminopyridines and glutaric acid." *Structural Chemistry*, Vol.27, no. 4, pp. 1303-1315, 2016.DOI 10.1007/s11224-016-0781-2
- [10] James E. Toney, "Photoluminescence Spectroscopy" in *Characterization of Materials*, 1st ed., Vol. 2, pp. 681-688, Spire Corporation, Bedford, Massachusetts; Published online: October 15, 2002; DOI: 10.1002/0471266965.com058.
- [11] Spackman, Mark A., and Dylan Jayatilaka. "Hirshfeld surface analysis." *CrystEngComm* 11, no. 1, pp.19-32, 2009.
- [12] McKinnon, Joshua J., Dylan Jayatilaka, and Mark A. Spackman. "Towards quantitative analysis of intermolecular interactions with Hirshfeld surfaces." *Chemical Communications*, 37, pp.3814-3816, 2007. doi:10.1039/b704980c.
- [13] Sudharsana, N., V. Krishnakumar, and R. Nagalakshmi. "Synthesis, experimental and theoretical Studies of 8-hydroxyquinolinium 3, 5-dinitrobenzoate single crystal." *Journal of Crystal Growth*, 398 pp. 45-57, 2014. (http://dx.doi.org/10.1016/j.jcrysgro.2014.03.051).
- [14] Seminario, Jorge M., ed. Recent developments and applications of modern density functional theory. Vol. 4. *Elsevier*, pp. 800-806, 1996.
- [15] Murray, Jane S., and Kalidas Sen, eds. Molecular electrostatic potentials: concepts and applications. Vol. 3. *Elsevier*, 1996.
- [16] Snehalatha, M., C. Ravikumar, I. Hubert Joe, N. Sekar, and V. S. Jayakumar. "Spectroscopic analysis and DFT calculations of a food additive Carmoisine." *Spectrochimica Acta Part A: Molecular and Biomolecular Spectroscopy*, Vol. 72, no. 3 pp. 654-662, 2009.doi.org/10.1016/j.saa.2008.11.017